Chemical Science

ROYAL SOCIETY OF CHEMISTRY

EDGE ARTICLE

View Article Online
View Journal | View Issue

Cite this: *Chem. Sci.*, 2025, **16**, 19683

All publication charges for this article have been paid for by the Royal Society of Chemistry

Catalytic enantioselective construction of two N-stereogenic centers of *ethano*- and *propano*-Tröger's bases

Chun-Yan Guan,[a] Tao Lu,[a] Ya Li,[a] Chao-Hua Liu,[a] Xiao Xiao[d] and Guang-Jian Mei *[abc]

Received 2nd August 2025
Accepted 23rd September 2025

DOI: 10.1039/d5sc05846e

rsc.li/chemical-science

Whereas enantioselective methods for constructing carbon stereocenters have been well established, those for creating heteroatomic stereocenters have received less attention. Nitrogen is the most abundant element in the Earth's atmosphere and plays an important role in the biochemical and physiological processes of organisms. However, owing to its rapid pyramidal inversion under general conditions, its stereochemistry has long been overlooked. Here, we report the catalytic enantioselective construction of two conformationally stable N-stereogenic centers of *ethano*- and *propano*-Tröger's bases. By using a Pd-catalyzed asymmetric annulative allylic alkylation reaction, various N-chiral *ethano*- and *propano*-TBs have been readily prepared in good yields with excellent enantioselectivities. Mechanistic investigations have shown that the two N-stereogenic centers are simultaneously established during intramolecular bridge formation. Furthermore, the synthesized TB products can serve as both an organo-catalyst for the aziridination reaction and a fluorescent/chiroptical probe for pH measurement.

Introduction

The control of molecular chirality remains a focus of modern synthetic chemistry. Since the early 20th century, synthetic chemists have been dedicated to developing catalytic asymmetric strategies to achieve efficient and precise synthesis of chiral molecules. Compared with the extensive exploration of creating conformationally and configurationally locked tetrahedral carbon (C) stereocenters, the enantioselective construction of heteroatomic stereocenters has garnered less attention (Fig. 1A).[1–5] Although nitrogen (N) is the most abundant element in the Earth's atmosphere and plays an important role in the biochemical and physiological processes of organisms, its stereochemistry has long been overlooked due to rapid pyramidal inversion under general conditions (Fig. 1B).[6–8] Quaternization to form ammonium cations can prevent this inversion by locking the configuration of the nitrogen stereocenter, but only for some structurally special amine *N*-oxides[9] and *N*-centered quaternary ammonium salts.[10,11] Alternatively, stable nitrogen stereocenters can be established in rigid cyclic tertiary amine structures, as ring tension can slow down or prevent the inversion of nitrogen's electron lone pair.[12–14]

Tröger's base (TB) is a fascinating tertiary amine with a rigid bicyclic skeleton (Fig. 1C).[15–19] In terms of stereochemistry, TB is known as the first N-chiral compound to be resolved and has become a classic example of "chiral nitrogen" in many stereochemistry textbooks.[20,21] In addition, the two aromatic rings orient in a nearly perpendicular fashion, making TB a cleft-like V-shaped molecule with a hydrophobic cavity. Hence, TB has attracted widespread attention in the fields of molecular recognition, supramolecular chemistry, and materials science.[22–24] However, TB undergoes racemization through a ring-opened achiral methylene-iminium intermediate under acidic conditions,[25–27] which is an obstacle for its intended use as a chiral ligand or catalyst in asymmetric catalysis.[28–30] One opportunity to address this issue is bridge modification, which increases the number of atoms strapping the two bridgehead N-atoms, avoiding the conventional racemization pathway *via* reversible aminalization.[31,32] In this context, Lacour *et al.* reported a highly enantiospecific synthesis of *ethano*-TBs from enantiopure TBs *via* rhodium(II)-catalyzed [1,2]-Stevens rearrangement.[33,34] Nevertheless, a general strategy for the direct catalytic enantioselective synthesis of configurationally stable TB analogues continues to be an attractive yet challenging goal in terms of the simultaneous construction of two bridgehead stereogenic N-atoms.[35–38]

The asymmetric allylic alkylation reaction is one of the most reliable methods for carbon–carbon and carbon–heteroatom

[a]*College of Chemistry, Zhengzhou University, Zhengzhou 450001, China. E-mail: meigj@zzu.edu.cn*
[b]*State Key Laboratory of Green Pesticides, Guizhou University, Guiyang 550025, China*
[c]*Pingyuan Laboratory (Zhengzhou University), Zhengzhou 450001, China*
[d]*Collaborative Innovation Center of Yangtze River Delta Region Green Pharmaceuticals, Zhejiang University of Technology, Hangzhou 310014, China*

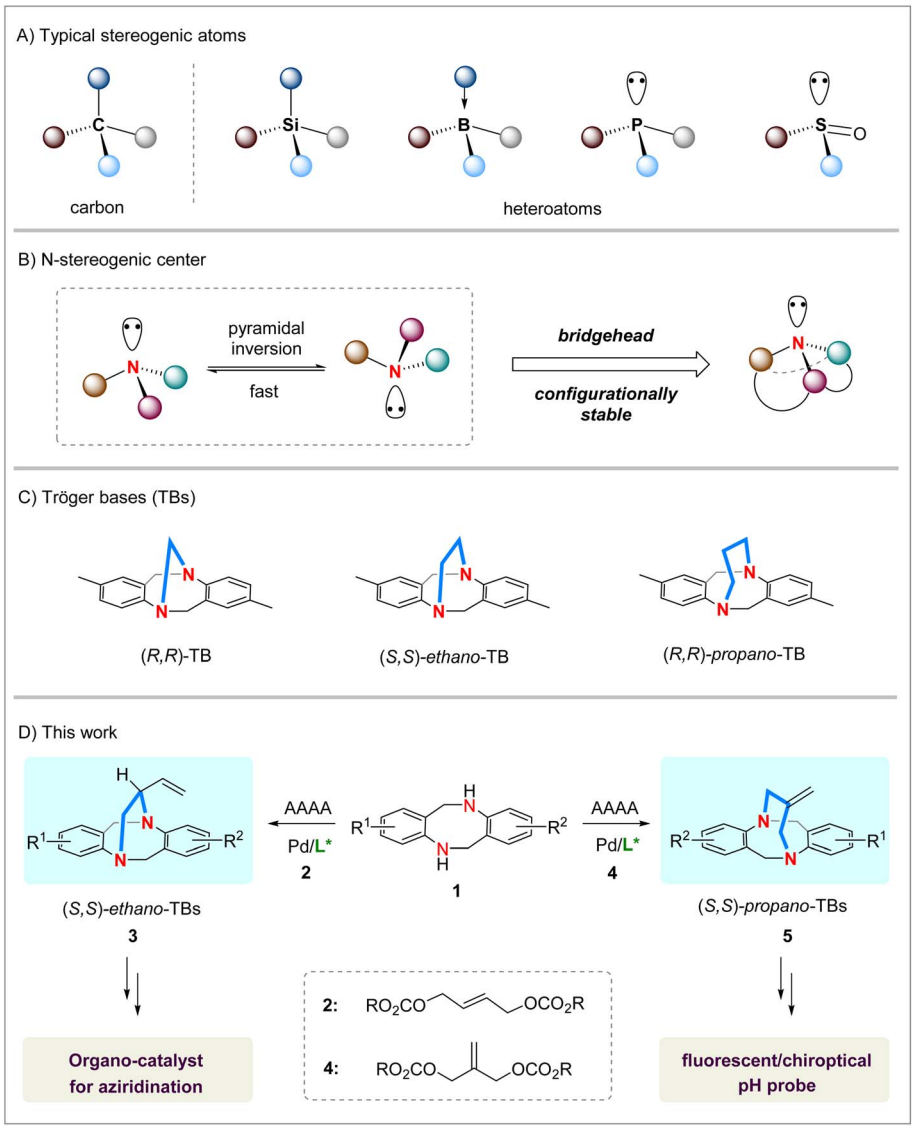

Fig. 1 Catalytic enantioselective synthesis of N-chiral *ethano*- and *propano*-TBs.

bond formation.[39–44] A notable advancement is its annulative version, which consists of a metal-catalyzed asymmetric annulative allylic alkylation (AAAA) reaction between dual nucleophiles and allylic diol derivatives and has become a powerful tool for preparing distinct chiral cyclic compounds.[45] Although significant advancements have been made in recent years,[46–50] to our knowledge, the AAAA reaction has been employed only to synthesize heterocycles with C-stereogenic centers. Our group has a long-term interest in the synthesis of multi-nitrogen-containing heterocycles.[51–56] Recently, we have achieved the enantioselective synthesis of TBs *via* chiral phosphoric acid (CPA)-catalyzed aminalization.[57] Here, we present a Pd-catalyzed AAAA reaction to construct N-stereogenic centers (Fig. 1D). The reactions of tetrahydrodibenzodiazocines (THDBDAs) **1** with butene dicarbonates **2** or isobutylene dicarbonates **4** are believed to proceed *via* a Pd-catalyzed cascade of two *N*-allylic alkylation reactions, in which two N-stereogenic centers are simultaneously established during intramolecular bridge formation. By using this method, a wide range of N-chiral *ethano*- and *propano*-TBs have been obtained in good yields with excellent enantioselectivities. The diversified late-manipulation of these bridged bicyclic products demonstrates their utility in organic synthesis. Furthermore, the synthesized *ethano*-TB can be directly used as an organo-catalyst for the aziridination reaction, and the H^+-induced fluorescence and electronic circular dichroism (ECD) responses of a *propano*-TB derivative suggest its potential application in pH fluorescent/chiroptical probes.

Table 1 Reaction optimization[a]

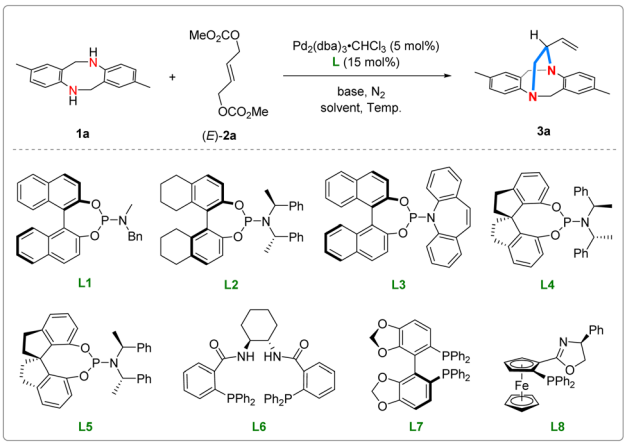

Entry	L	Solvent	Base	Temp./°C	Yield[b] (%)	ee[c] (%)
1	**L1**	CH_2Cl_2	Cs_2CO_3	35	65	25
2	**L2**	CH_2Cl_2	Cs_2CO_3	35	72	50
3	**L3**	CH_2Cl_2	Cs_2CO_3	35	56	37
4	**L4**	CH_2Cl_2	Cs_2CO_3	35	80	77
5	**L5**	CH_2Cl_2	Cs_2CO_3	35	85	89
6	**L6**	CH_2Cl_2	Cs_2CO_3	35	n.d.	—
7	**L7**	CH_2Cl_2	Cs_2CO_3	35	n.d.	—
8	**L8**	CH_2Cl_2	Cs_2CO_3	35	n.d.	—
9	**L5**	DCE	Cs_2CO_3	35	80	82
10	**L5**	$CHCl_3$	Cs_2CO_3	35	52	91
11	**L5**	$CHCl_3$	Na_2CO_3	35	86	95
12	**L5**	$CHCl_3$	K_2CO_3	35	81	92
13	**L5**	$CHCl_3$	KO^{t}Bu	35	85	90
14	**L5**	$CHCl_3$	DIPEA	35	83	92
15	**L5**	$CHCl_3$	Na_2CO_3	20	81	95
16	**L5**	$CHCl_3$	Na_2CO_3	40	86	96
17	**L5**	$CHCl_3$	Na_2CO_3	60	90	96

[a] Unless otherwise indicated, the reaction conditions were as follows: **1a** (0.05 mmol, 1 equiv.), **2** (0.075 mmol, 1.5 equiv.), $Pd_2(dba)_3 \cdot CHCl_3$ (5 mol%), **L** (15 mol%), and base (0.1 mmol, 2 equiv.) in the specified solvent at the given temperature for 24 h, all dr > 20 : 1. [b] Isolated yield. [c] Determined by chiral HPLC analysis. n.d. = not detected.

Results and discussion

We initiated the investigation with a model reaction between THDBDA **1a** and (*E*)-butene dicarbonate **2a** (Table 1). To our delight, by employing chiral phosphoramidite ligands, the projected AAAA reaction readily took place in CH_2Cl_2, affording the desired product *ethano*-TB **3a** (entries 1–5). Among them, BINOL-derived ligands (**L1**, **L2**, and **L3**) furnished **3a** in moderate yields and enantioselectivities (entries 1–3). When the backbone is changed to spiro-diol (**L4** and **L5**), the *ee* value can be improved to a good level (entries 4–5). Phosphine ligands (**L6**, **L7**, and **L8**) were ineffective for this reaction (entries 6–8). The solvent effect was then studied, and chloroform provided **3a** with 91% *ee* (entry 10). Several commonly used inorganic and organic bases were subsequently screened (entries 11–14). While they were all effective, Na_2CO_3 was identified as the best choice (entry 11). The reaction temperature had some impact on the yield (entries 15–17). At 60 °C, product **3a** was obtained in 90% yield with 96% *ee*. Notably, only one diastereoisomer was observed during the investigation (all dr > 20 : 1).

Under the best conditions, we examined the substrate generality of the Pd-catalyzed AAAA reaction (Fig. 2). The reaction conditions were compatible with various 2-butenylene dicarbonates (**2a–d**), which afforded **3a** with consistently excellent enantioselectivity. We next investigated the effect of different substituents on the phenyl ring of THDBDAs **1**. Alkyl groups at the 2(8)-position, such as ethyl (**3b**), *n*-propyl (**3c**), *i*-propyl (**3d**), *n*-butyl (**3e**), *t*-butyl (**3f**), *n*-amyl (**3g**), and benzyl (**3h**) groups, were well tolerated, providing the corresponding products in good yields (75–91%) with excellent enantioselectivities (93–97%). However, other types of substituents afforded delicate effects. When phenyl substituted THDBDA was employed, the corresponding product **3i** was obtained in 80% yield with 90% *ee*. Unsubstituted THDBDA was suitable for this reaction, but the enantioselectivity was slightly reduced (**3j**). For the halogen substituents, the fluoro group (**3k**) provided a higher *ee* value than the chloro group (**3l**). Electron-donating groups such as SMe (**3m**), OMe (**3n**), and OBn (**3o**) were also compatible. Nevertheless, the reaction was applicable to THDBDAs bearing alkyl substituents, including methyl (**3p**), ethyl (**3q**), *i*-propyl (**3r′**), and *t*-butyl (**3s′**) groups, at the 3(9)-position. However, owing to unfavorable steric effects, the substituent at the 4(10)-position was not conducive to enantiocontrol, as exemplified in **3t**. In a previous report on Tröger's bases, Lenev, Buss, and Kostyanovsky *et al.* demonstrated that the bis-*ortho*-substitution of the aromatic groups next to the nitrogen atoms dramatically increased the racemization barrier of the stereogenic nitrogen.[58] Di- and trisubstituted THDBDAs were employed as suitable substrates, leading to the formation of products **3u–x** in ≥83% yields with up to 95% *ee*. When (hetero)ring-fused substrates (**3y** and **3z**) were utilized, consistently good yields and excellent enantioselectivities were obtained. The use of unsymmetrical substrates resulted in the formation of **3a′** as a pair of diastereoisomers, which may be attributed to the regioselective allylic alkylation of the two amino groups on the two electronically differentiated aromatic rings. The absolute configuration of **3r′** was determined *via* X-ray crystallographic analysis.

Encouraged by the successful synthesis of N-chiral *ethano*-TBs, we decided to apply this Pd-catalyzed AAAA reaction to prepare N-chiral *propano*-TBs. This structural variation is highly valuable as it could lead to a dramatic change in the shape of the TB scaffold.[31] Despite its appeal, strapping two bridgehead nitrogens with three atoms is highly challenging.[59] Under standard conditions, the projected reaction of THDBDA **1a** with isobutylene dicarbonate **4a** readily occurred to yield *propano*-TB

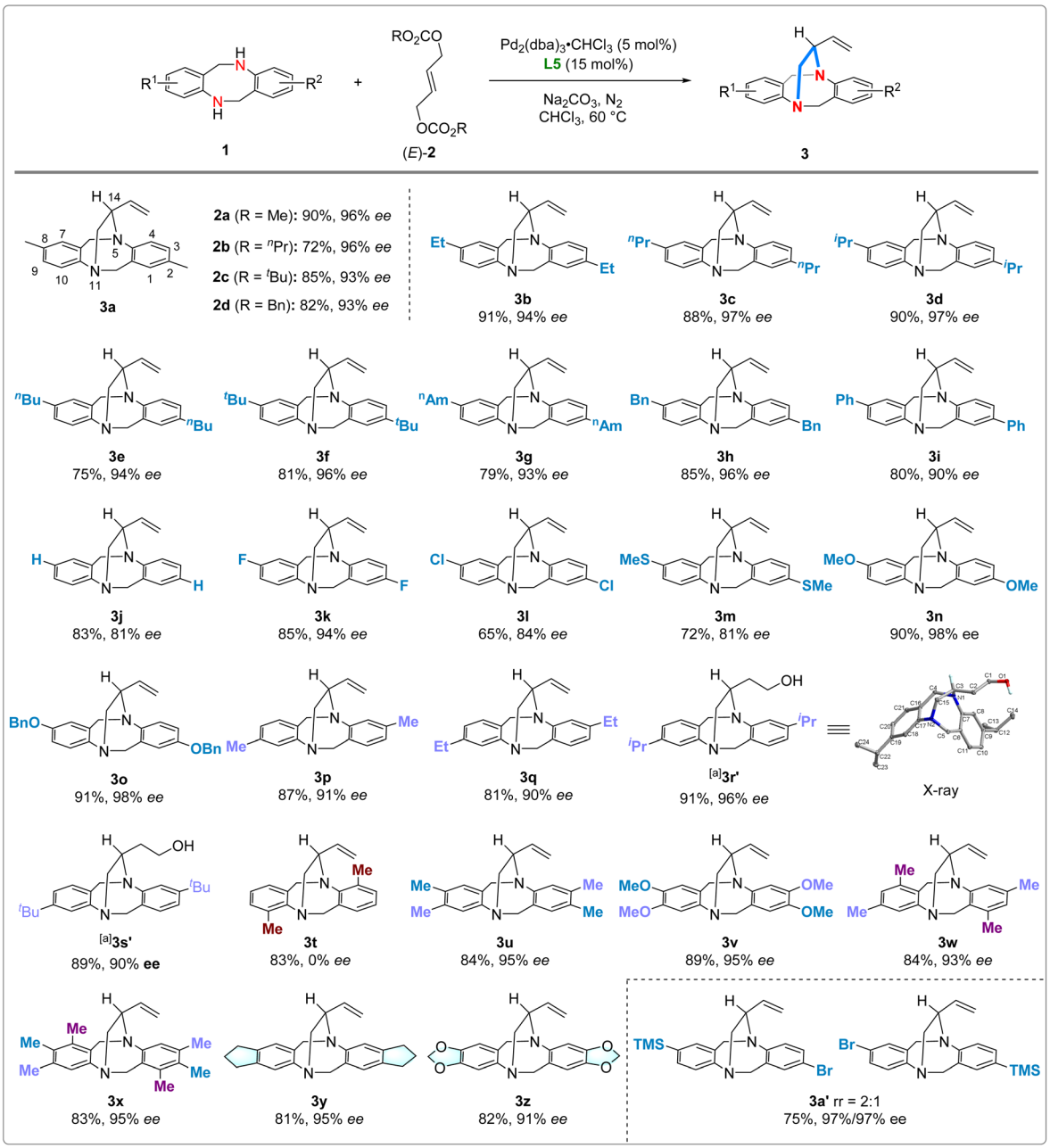

Fig. 2 Substrate scope of *ethano*-TBs. Unless otherwise indicated, the reaction conditions were as follows: **1** (0.1 mmol, 1 equiv.), **2** (0.15 mmol, 1.5 equiv.), $Pd_2(dba)_3 \cdot CHCl_3$ (5 mol%), **L5** (15 mol%), and Na_2CO_3 (0.2 mmol, 2 equiv.) in $CHCl_3$ (1 mL) under a N_2 atmosphere at 60 °C for 24 h, all dr > 20 : 1. [a] Followed by hydroboration–oxidation.

5a with moderate enantioselectivity. By further optimizing the reaction conditions (see the SI for details), **L1** was selected as the best ligand, and the reaction temperature was set to −10 °C, which afforded **5a** in 78% yield with 90% *ee*. Subsequently, the substrate scope was examined, and the results are summarized in Fig. 3. The ester group of isobutylene dicarbonates **4** can be varied, from Me (**4a**), ^{n}Pr (**4b**), ^{t}Bu (**4c**), to Bn (**4d**), with consistently high yields and excellent *ee* values. At the 2(8)-position of THDBDA, different types of substituents, including electron-neutral hydrogen, electron-donating alkyl and alkoxy groups, and electron-withdrawing halo groups, were well tolerated, providing *propano*-TBs **5b–5i** in 65–91% yields with 92–97% *ee*. The alkyl substituents at the 3(9)-position appeared to be inconsequential to the reaction results, and excellent

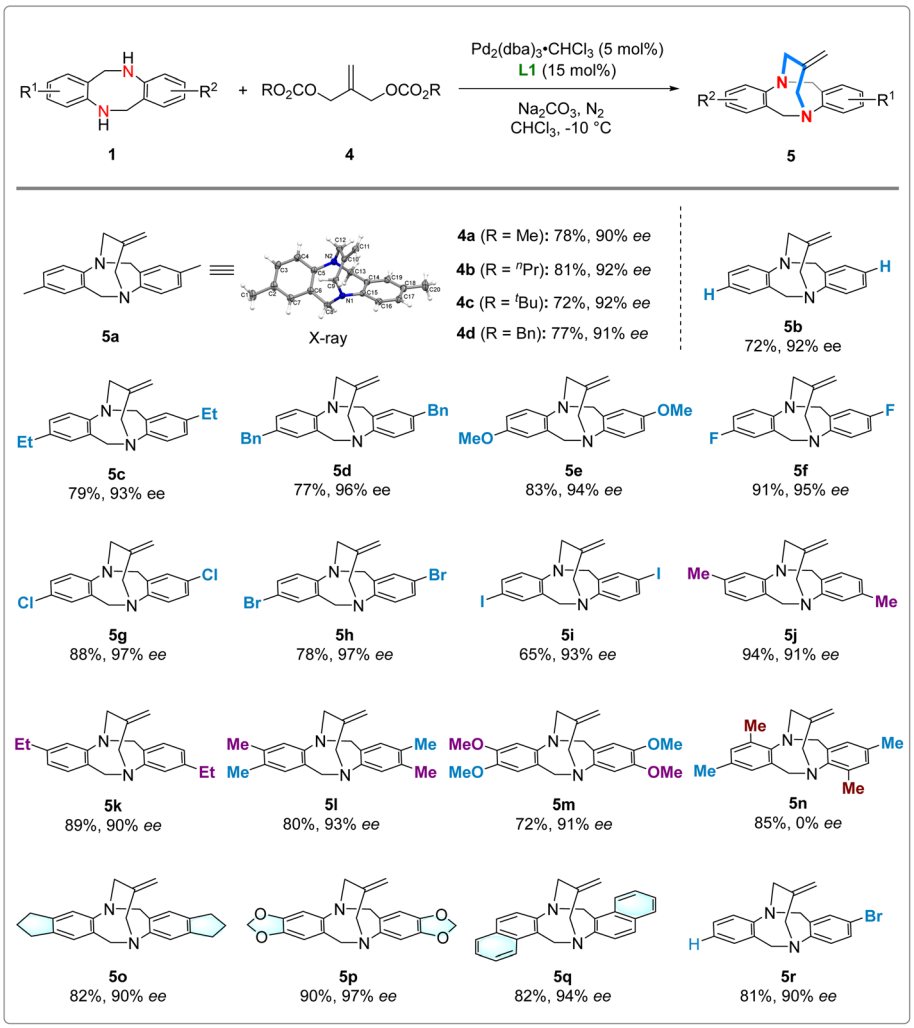

Fig. 3 Substrate scope of *propano*-TBs. Unless otherwise indicated, the reaction conditions were as follows: **1** (0.1 mmol, 1 equiv.), **4** (0.15 mmol, 1.5 equiv.), $Pd_2(dba)_3 \cdot CHCl_3$ (5 mol%), **L1** (15 mol%), and Na_2CO_3 (0.2 mmol, 2 equiv.) in $CHCl_3$ (1 mL) under a N_2 atmosphere at −10 °C for 18 h.

enantioselectivity was retained (**5j** and **5k**). In particular, we examined the tolerance of the reaction to disubstituted substrates. While **5l** and **5m** were formed with 91% *ee*, racemic **5n** was obtained presumably due to the unfavourable steric hindrance at the 5(10)-position. The reaction was also applicable to (hetero)ring-fused and unsymmetrical THDBDAs, delivering **5o–5r** in 81–90% yields with 90–97% *ee*. The absolute configuration of **5a** was determined *via* X-ray crystallographic analysis.

To gain mechanistic insight, control experiments were performed (Fig. 4A). Both (*E*)- and (*Z*)-butene dicarbonates were subjected to the reaction under standard reaction conditions. The observed difference in the enantioselectivity of **3a** indicated a mismatched relationship between the (*Z*)-double bond and chiral ligand. A nonlinear effect (NLE) study on the reaction of **1a** with **2b** was performed (Fig. 4B). A (+)-NLE effect was obtained, which indicated that in the reactive chiral Pd-complex, the palladium and ligand may be not present in a 1 : 1 ratio. However, given the relatively weak effect, other chiral perturbations, including reservoir effects, cannot be ruled out. Furthermore, to confirm the involvement of a tandem double alkylation process, we carried out stepwise experiments (Fig. 4C). Monoalkylated products **7** or **9** were pre-synthesized *via* the alkylation of **1a** with allyl bromides **6** or **8**. Under standard conditions, **7** and **9** were readily converted to *ethano*-TB **3a** and *propano*-TB **5a** in good yields with excellent enantioselectivities, respectively, proving that the monoalkylated product might be a viable intermediate in the tandem process. On the basis of the experimental results above and those of previous studies,[60–64] a plausible catalytic cycle for the synthesis of *ethano*-TB **3a** is depicted in Fig. 4D (left). Treatment of the chiral Pd-complex generated *in situ* with (*E*)-butene dicarbonate

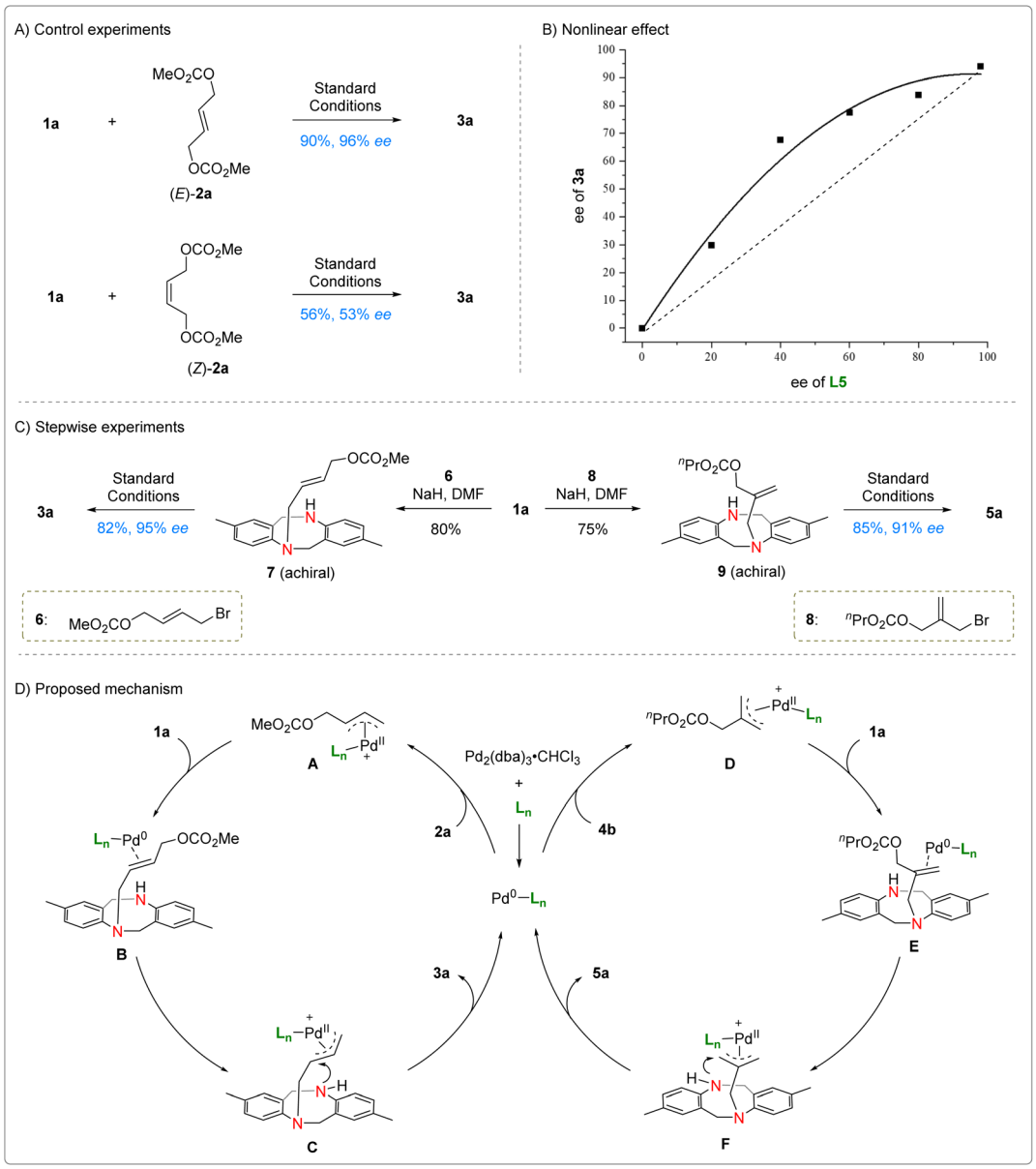

Fig. 4 Mechanistic considerations.

2a leads to a decarboxylative process, affording Pd(II)-π–allyl intermediate A. Subsequent allylation with **1a** gives mono-alkylated intermediate **B**, enabling a secondary decarboxylative process to form Pd(II)-π–allyl intermediate **C**. The subsequent intramolecular allylation completes the entire catalytic cycle, regenerating the chiral Pd(0) catalyst for the next catalytic cycle and forming product **3a**. The reaction of **1a** with isobutylene dicarbonate **4a** involves a similar catalytic cycle (Fig. 4D, right) to afford *propano*-TB **5a**.

Finally, further transformations and downstream applications were performed to demonstrate the synthetic utility of this protocol (Fig. 5). Under standard conditions, the large-scale syntheses of **3n** and **5a** proceeded smoothly and maintained excellent enantioselectivities (see the SI for details). Moreover, late-stage manipulations (Fig. 5A), such as hydrogenation (**10**) and deprotection (**11**), of *ethano*-TB **3n** were readily conducted without erosion of enantiomeric purity. The terminal olefin underwent a standard hydroboration–oxidation reaction to yield alcohol **12** with excellent enantioselectivity (98% *ee*). The subsequent bromination and azidation reactions enabled the formation of bromide **13** and azide **14**. The newly formed hydroxyl and azide groups are modifiable sites. For instance,

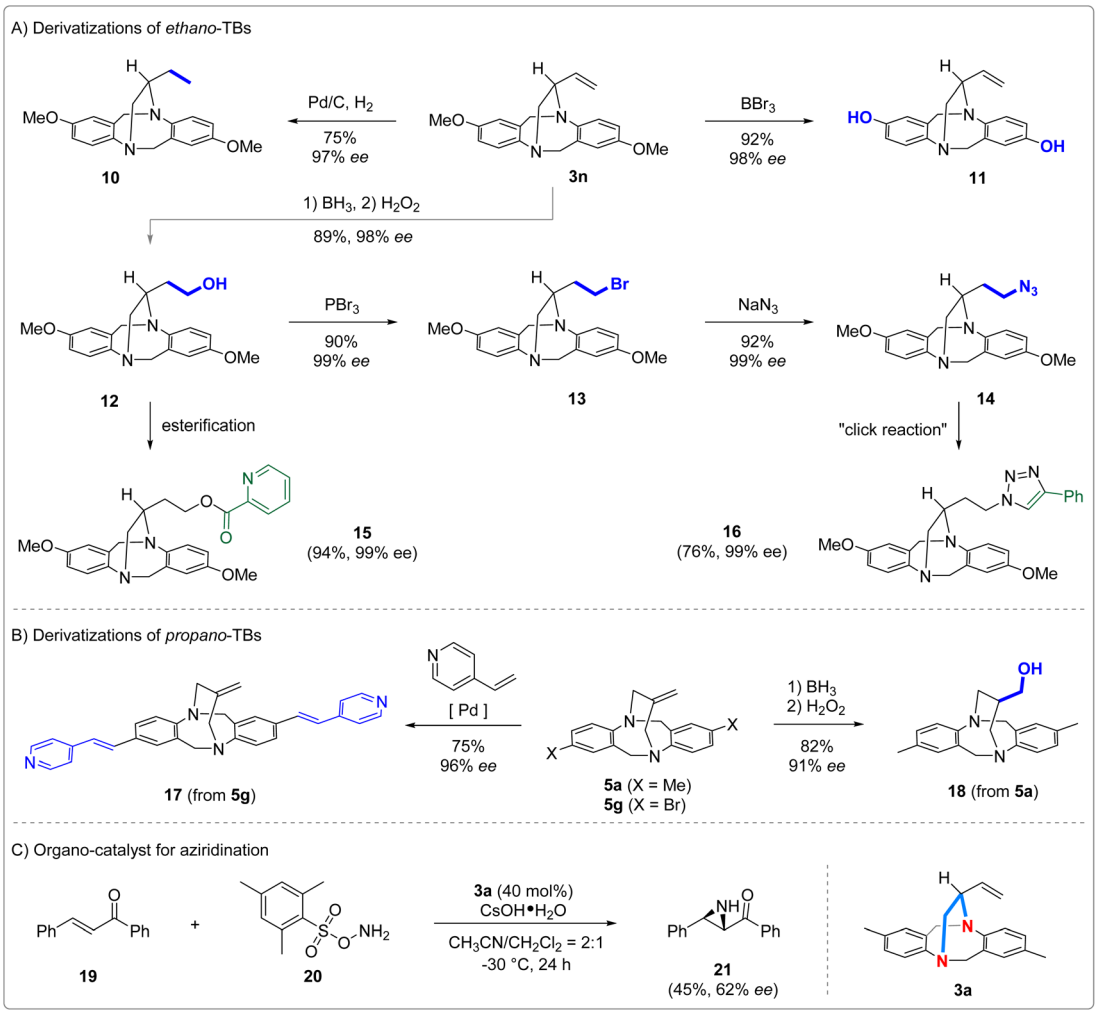

Fig. 5 Further transformations and downstream applications.

esterification with 2-picolinic acid led to *ethano*-TB derivative **15** with a potential coordination site for ligand design, and a "click reaction" with acetylene resulted in *ethano*-TB-triazole **16**. On the other hand, late-stage functionalization can also be carried out on the benzene ring or double bond of *propano*-TB (Fig. 5B). For example, **5g** can undergo a Heck coupling reaction with 4-vinylpyridine to produce conjugated alkene **17**, and hydroboration–oxidation of **5a** delivers alcohol **18**. In addition, *ethano*-TB **3a** can promote the enantioselective aziridination of chalcones, which demonstrates the potential of these configurationally stable *ethano*-TBs for asymmetric catalysis (Fig. 5C).[28]

By incorporating an electron-donating amine moiety and an electron-accepting pyridine group, *propano*-TB derivative **17** exhibited an intramolecular charge transfer effect (Fig. 6).[65] As shown in Fig. 6, the UV-vis absorption and fluorescence emission spectra of compound (−)-**17** were measured under various acidic conditions. Along with H^+ addition, the original absorption band at 330 nm decreased and a new band around 410 nm increased gradually (Fig. 6A). The fluorescence measurements were carried out with an excitation wavelength of 375 nm. Similarly, with the addition of an acid, the original emission band at 470 nm disappeared, and a new band emerged at approximately 550 nm (Fig. 6B). A notable fluorescence colour change from blue to yellow was observed with increasing acidity. Furthermore, the circular dichroism (CD) spectra of (−)-**17** as a function of pH are displayed in Fig. 6C. Upon increasing the amount of H^+, the original absorption band at 275 nm decreased, whereas the new absorption band near 310 nm gradually increased. Such fluorescence emission and circularly polarized light absorption properties enable TB derivative **17** to serve as a highly sensitive probe for pH measurement in acidic regions through fluorometric and chiroptical changes.

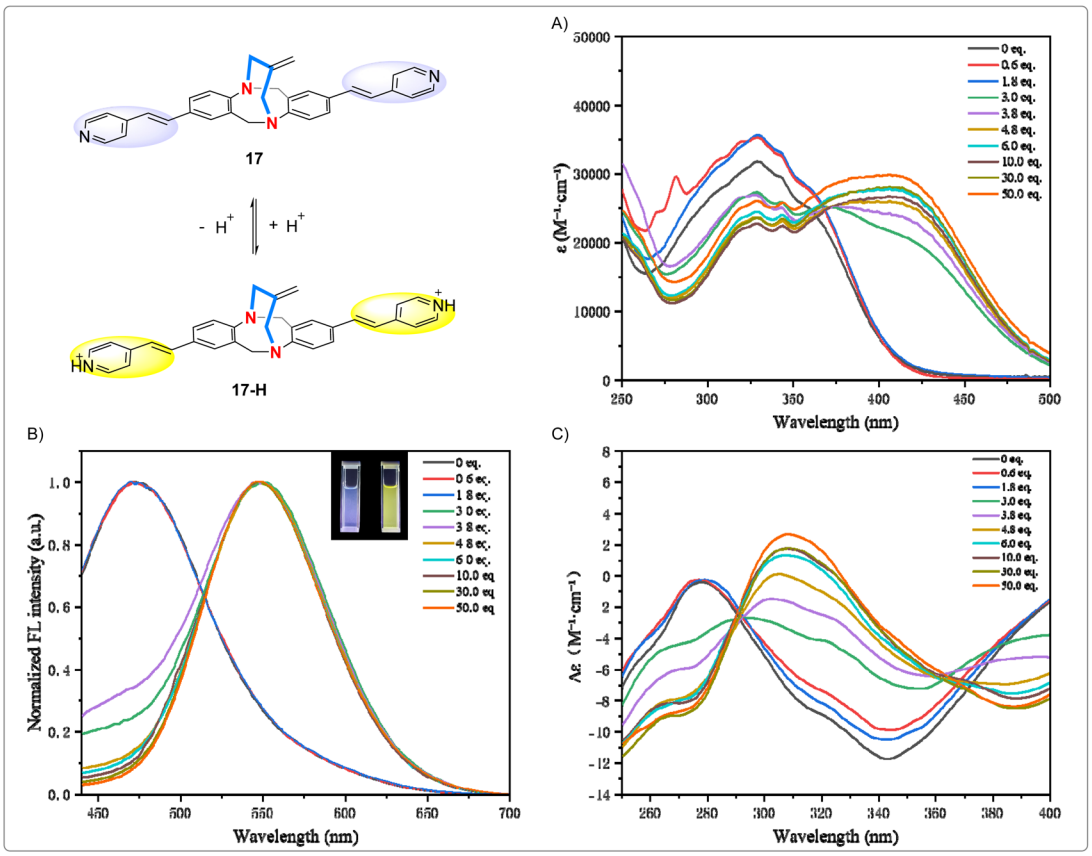

Fig. 6 Switchable photophysical and chiroptical properties. (A) UV/Vis absorption spectra, ε, molar extinction coefficient, (B) fluorescence spectra, and (C) circular dichroism (CD) spectra, $\Delta\varepsilon$, molar circular dichroism. (−)-**17** + TFA (× eq.) in MeOH at 25 °C, 2×10^{-5} M.

Conclusions

In conclusion, we constructed two N-stereogenic centers in *ethano*- and *propano*-Tröger's bases *via* a Pd-catalyzed asymmetric annulative allylic alkylation reaction. Control and stepwise experiments prove that the reaction cascade of tetrahydrodibenzodiazocines with butene dicarbonates or isobutylene dicarbonates proceeds *via* two tandem Pd-catalyzed *N*-allylic alkylation reactions and that the two N-stereogenic centers are simultaneously established during intramolecular bridge formation. A wide range of N-chiral *ethano*- and *propano*-TBs have been readily prepared in good yields with excellent enantioselectivities. The diversified late-manipulation of these bridged bicyclic products demonstrates their utility in organic synthesis. Furthermore, the synthesized *ethano*-TB can be used downstream as an organo-catalyst for the aziridination reaction, and the H^+-induced fluorescence emission and circularly polarized light absorption responses of a *propano*-TB derivative enable it to work as a fluorescent/chiroptical probe for pH measurement in acidic regions. Along this line, further investigations on the construction of N-stereogenic centers are ongoing in our laboratory and will be reported in due course.

Author contributions

C.-Y. G., T. L., Y. L., C.-H. L., and X. X. performed and analyzed the experiments. G.-J. M. conceived and designed the project. G.-J. M. overall supervised the project. All authors prepared this manuscript.

Conflicts of interest

We have filed a patent application related to this work (application no. CN119350350A, filed on January 24, 2025). The patent is currently under review and has not yet been granted. The authors declare no other competing interests.

Data availability

CCDC 2390173 (**3r′**) and 2446125 (**5a**) contain the supplementary crystallographic data for this paper.[66a,b]

The authors declare that the data relating to the characterization of products, experimental protocols and the computational studies are available within the article and its supplementary information (SI). Supplementary information:

original NMR spectra of products **3–21**. See DOI: https://doi.org/10.1039/d5sc05846e.

Acknowledgements

The authors acknowledge the financial support from the National Natural Science Foundation of China (22371265 and 22208302), Natural Science Foundation of Henan Province (232301420047), and the project of State Key Laboratory of Green Pesticide, Guizhou Medical University (GPLKF202507).

Notes and references

1 Y.-M. Cui, Y. Lin and L.-W. Xu, Catalytic synthesis of chiral organoheteroatom compounds of silicon, phosphorus, and sulfur *via* asymmetric transition metal-catalyzed C–H functionalization, *Coord. Chem. Rev.*, 2017, **330**, 37–52.

2 J. Diesel and N. Cramer, Generation of Heteroatom Stereocenters by Enantioselective C–H Functionalization, *ACS Catal.*, 2019, **9**, 9164–9177.

3 X. Ye, L. Peng, X. Bao, C.-H. Tan and H. Wang, Recent developments in highly efficient construction of P-stereogenic centers, *Green Synth. Catal.*, 2021, **2**, 6–18.

4 Y. Xia, B. Xu, Z. Zhang and J. Zhang, Pd/Ag dual-catalyzed asymmetric synthesis of sulfur-stereogenic sulfoximines *via* enantioselective intramolecular C–H arylation, *Green Synth. Catal.*, 2025, DOI: 10.1016/j.gresc.2025.06.004.

5 B. Dong, J. Zhang, X.-Y. Ye, X. Huang and Y. R. Chi, Catalytic construction of P-stereogenic center *via* phosphorus-centered nucleophilic substitution, *Chin. Chem. Lett.*, 2025, **36**, 111052.

6 J. M. Lehn, Nitrogen inversion, *Fortschr. Chem. Forsch.*, 1970, **15**, 311–377.

7 A. Rauk, L. C. Allen and K. Mislow, Pyramidal Inversion, *Angew. Chem., Int. Ed.*, 1970, **9**, 400–414.

8 R. Zhang, S. Xu, Z. Luo, Y. Liu and J. Zhang, Enantiodivergent Hydrogenation of Exocyclic α,β-Unsaturated Lactams Enabled by Switching the N-Chirality of Iridium Catalyst, *Angew. Chem., Int. Ed.*, 2023, **62**, e202213600.

9 S. Bhadra and H. Yamamoto, Catalytic Asymmetric Synthesis of N-Chiral Amine Oxides, *Angew. Chem., Int. Ed.*, 2016, **55**, 13043–13046.

10 M. P. Walsh, J. M. Phelps, M. E. Lennon, D. S. Yufit and M. O. Kitching, Enantioselective synthesis of ammonium cations, *Nature*, 2021, **597**, 70–76.

11 Z. Luo, M. Liao, W. Li, S. Zhao, K. Tang, P. Zheng, Y. R. Chi, X. Zhang and X. Wu, Ionic Hydrogen Bond-Assisted Catalytic Construction of Nitrogen Stereogenic Center *via* Formal Desymmetrization of Remote Diols, *Angew. Chem., Int. Ed.*, 2024, **63**, e202404979.

12 S. Huang, H. Wen, Y. Tian, P. Wang, W. Qin and H. Yan, Organocatalytic Enantioselective Construction of Chiral Azepine Skeleton Bearing Multiple-Stereogenic Elements, *Angew. Chem., Int. Ed.*, 2021, **60**, 21486–21493.

13 C. Ma, Y. Sun, J. Yang, H. Guo and J. Zhang, Catalytic Asymmetric Synthesis of Tröger's Base Analogues with Nitrogen Stereocenter, *ACS Cent. Sci.*, 2023, **9**, 64–71.

14 T. Yu, S. Cheng, Y. Luo, J. Li, Y. Liang, S. Luo and Q. Zhu, Immobilizing Stereogenic Nitrogen Center in Doubly Fused Triarylamines through Palladium-Catalyzed Asymmetric C–H Activation/Seven-Membered-Ring Formation, *ACS Catal.*, 2023, **13**, 9688–9694.

15 F. Vögtle, *Fascinating molecules in organic chemistry*, Wiley, 1992, p. 304.

16 M. Valík, R. M. Strongin and V. Král, Tröger's Base Derivatives—New Life for Old Compounds, *Supramol. Chem.*, 2005, **17**, 347–367.

17 B. Dolenský, J. Elguero, V. Král, C. Pardo and M. Valík, Current Tröger's Base Chemistry, *Adv. Heterocycl. Chem.*, 2007, **93**, 1–56.

18 S. Sergeyev, Recent Developments in Synthetic Chemistry, Chiral Separations, and Applications of Tröger's Base Analogues, *Helv. Chim. Acta*, 2009, **92**, 415–444.

19 Ö. V. Rúnarsson, J. Artacho and K. Wärnmark, The 125thAnniversary of the Tröger's Base Molecule: Synthesis and Applications of Tröger's Base Analogues, *Eur. J. Org Chem.*, 2012, **2012**, 7015–7041.

20 J. Tröger, Ueber einige mittelst nascirenden Formaldehydes entstehende Basen, *J. Prakt. Chem.*, 1887, (36), 225–245.

21 V. Prelog and P. Wieland, Über die Spaltung der Tröger'schen Base in optische Antipoden, ein Beitrag zur Stereochemie des dreiwertigen Stickstoffs, *Helv. Chim. Acta*, 1944, **27**, 1127–1134.

22 B. Dolenský, M. Havlík and V. Král, Oligo Tröger's bases—new molecular scaffolds, *Chem. Soc. Rev.*, 2012, **41**, 3839.

23 Q. Xu, B. Xin, J. Wei, Y. Ma, Z. Qing, C. Feng, S. Yi, N. Li, K. Li, F. Wang, J. Zhao, L. Yang, L. Yao, W. Jiang, Y. Dai and Z. Dai, Troger's base polymeric membranes for CO2 separation: a review, *J. Mater. Chem. A*, 2023, **11**, 15600–15634.

24 C. Shi, G. Xu, H. Qiu, Y. Li, X. Lu, J. Jiang and L. Wang, Tröger's base-embedded macrocycles with chirality, *Chem. Commun.*, 2025, **61**, 2450–2467.

25 A. Greenberg, N. Molinaro and M. Lang, Structure and dynamics of Troeger's base and simple derivatives in acidic media, *J. Org. Chem.*, 1984, **49**, 1127–1130.

26 O. Trapp, G. Trapp, J. Kong, U. Hahn, F. Vögtle and V. Schurig, Probing the Stereointegrity of Tröger's Base—A Dynamic Electrokinetic Chromatographic Study, *Chem.–Eur. J.*, 2002, **8**, 3629.

27 D. A. Lenev, K. A. Lyssenko, D. G. Golovanov, V. Buss and R. G. Kostyanovsky, Bis-ortho-Substitution by Methyl Groups Dramatically Increases the Racemization Barrier of Tröger Bases, *Chem.–Eur. J.*, 2006, **12**, 6412–6418.

28 Y. M. Shen, M. X. Zhao, J. Xu and Y. Shi, An Amine-Promoted Aziridination of Chalcones, *Angew. Chem., Int. Ed.*, 2006, **45**, 8005–8008.

29 M. S. Sigman and D. R. Jensen, Ligand-Modulated Palladium-Catalyzed Aerobic Alcohol Oxidations, *Acc. Chem. Res.*, 2006, **39**, 221–229.

30 M. Harmata, K.-O. Rayanil and C. L. Barnes, Sequential Alkylation of Tröger's Base. An Approach to New Chiral Ligands, *Supramol. Chem.*, 2007, **18**, 581–586.

31 M. Faroughi, A. C. Try, J. Klepetko and P. Turner, Changing the shape of Tröger's base, *Tetrahedron Lett.*, 2007, **48**, 6548–6551.
32 R. Pereira, J. Wolstenhulme, G. Sandford, T. D. Claridge, V. Gouverneur and J. Cvengros, Synthesis and characterization of a novel N-F reagent derived from the ethano-Troger's base: (1)J(FN) coupling constants as a signature for the N-F bond, *Chem. Commun.*, 2016, **52**, 1606–1609.
33 A. Sharma, L. Guénée, J. V. Naubron and J. Lacour, One-Step Catalytic Asymmetric Synthesis of Configurationally Stable Tröger Bases, *Angew. Chem., Int. Ed.*, 2011, **50**, 3677–3680.
34 A. Sharma, C. Besnard, L. Guénée and J. Lacour, Asymmetric synthesis of ethano-Tröger bases using CuTC-catalyzed diazo decomposition reactions, *Org. Biomol. Chem.*, 2012, **10**, 966–969.
35 Y. Hamada and S. Mukai, Synthesis of Ethano-Troger's base, configurationally stable substitute of Troger's base, *Tetrahedron: Asymmetry*, 1996, **7**, 2671–2674.
36 D. A. Lenev, D. G. Golovanov, K. A. Lyssenko and R. G. Kostyanovsky, Configurationally stable methylates of methano- and ethano-Tröger bases, *Tetrahedron: Asymmetry*, 2006, **17**, 2191–2194.
37 C. Michon, A. Sharma, G. Bernardinelli, E. Francotte and J. Lacour, Stereoselective synthesis of configurationally stable functionalized ethano-bridged Tröger bases, *Chem. Commun.*, 2010, **46**, 2206.
38 S. A. Pujari, L. Guénée and J. Lacour, Efficient Synthesis of Imino-methano Tröger Bases by Nitrene Insertions into C–N Bonds, *Org. Lett.*, 2013, **15**, 3930–3933.
39 B. M. Trost and D. L. Van Vranken, Asymmetric Transition Metal-Catalyzed Allylic Alkylations, *Chem. Rev.*, 1996, **96**, 395–422.
40 N. A. Butt and W. B. Zhang, Transition metal-catalyzed allylic substitution reactions with unactivated allylic substrates, *Chem. Soc. Rev.*, 2015, **44**, 7929–7967.
41 Q. Cheng, H.-F. Tu, C. Zheng, J.-P. Qu, G. Helmchen and S.-L. You, Iridium-Catalyzed Asymmetric Allylic Substitution Reactions, *Chem. Rev.*, 2018, **119**, 1855–1969.
42 O. Pàmies, J. Margalef, S. Cañellas, J. James, E. Judge, P. J. Guiry, C. Moberg, J.-E. Bäckvall, A. Pfaltz, M. A. Pericàs and M. Diéguez, Recent Advances in Enantioselective Pd-Catalyzed Allylic Substitution: From Design to Applications, *Chem. Rev.*, 2021, **121**, 4373–4505.
43 D. Wang, J. Zong, B. Wang, L. Sun, X. Xiao, H. Piao, M. Ke and F. Chen, Asymmetric synthesis of allylic sulfonamides with axially and central chirality *via* palladium-catalyzed of atroposelective N-allylic alkylation, *Green Synth. Catal.*, 2025, **6**, 211–215.
44 M. Liu, H. Zhao and C. Li, Rh(I)-catalyzed regio- and enantioselective allylic alkylation of Meldrum's acid, *Chin. Chem. Lett.*, 2021, **32**, 385–388.
45 B. M. Trost and C. A. Kalnmals, Annulative Allylic Alkylation Reactions between Dual Electrophiles and Dual Nucleophiles: Applications in Complex Molecule Synthesis, *Chem.–Eur. J.*, 2019, **26**, 1906–1921.
46 B. M. Trost and G. Dong, New Class of Nucleophiles for Palladium-Catalyzed Asymmetric Allylic Alkylation. Total Synthesis of Agelastatin A, *J. Am. Chem. Soc.*, 2006, **128**, 6054–6055.
47 H. He, W. B. Liu, L. X. Dai and S. L. You, Enantioselective Synthesis of 2,3-Dihydro-1H-benzo[b]azepines: Iridium-Catalyzed Tandem Allylic Vinylation/Amination Reaction, *Angew. Chem., Int. Ed.*, 2010, **49**, 1496–1499.
48 Y. Zheng, S. Dong, K. Xu, D. Liu and W. Zhang, Pd-Catalyzed Asymmetric Allylic Substitution Cascade of Substituted 4-Hydroxy-2H-pyrones with meso-Allyl Dicarbonates, *Org. Lett.*, 2022, **24**, 3440–3444.
49 H.-L. Mao, Y.-X. Wang, X. Wang, H.-Y. Wang, W.-J. Hao and B. Jiang, Pd-Catalyzed Asymmetric Annulative Dearomatization of Phenols for Regio- and Enantioselective Synthesis of Spirocyclohexadienones, *Org. Lett.*, 2023, **25**, 5963–5968.
50 J. Xu, G. Wang, K. Ding and X. Wang, Dirhodium–Palladium Dual-Catalyzed [1 + 1 + 3] Annulation to Heterocycles Using Primary Amines or H2O as the Heteroatom Sources, *J. Am. Chem. Soc.*, 2025, **147**, 2000–2009.
51 Y.-H. Miao, Z.-X. Zhang, X.-Y. Huang, Y.-Z. Hua, S.-K. Jia, X. Xiao, M.-C. Wang, L.-P. Xu and G.-J. Mei, Catalytic asymmetric dearomative azo-Diels–Alder reaction of 2-vinlyindoles, *Chin. Chem. Lett.*, 2024, **35**, 108830.
52 C.-Y. Guan, S. Zou, C. Luo, Z.-Y. Li, M. Huang, L. Huang, X. Xiao, D. Wei, M.-C. Wang and G.-J. Mei, Catalytic asymmetric synthesis of planar-chiral dianthranilides *via* (Dynamic) kinetic resolution, *Nat. Commun.*, 2024, **15**, 4580.
53 Y.-D. Fu, H. Zhang, B.-B. Li, L. Huang, X. Xiao, M.-C. Wang, D. Wei and G.-J. Mei, Azocarboxamide-enabled enantioselective regiodivergent unsymmetrical 1,2-diaminations, *Nat. Commun.*, 2024, **15**, 10225.
54 C.-Y. Guan, T.-J. Han, S.-K. Jia, Y.-Z. Hua and G.-J. Mei, Diastereodivergent formal [4 + 1] cycloaddition of azoalkenes as one-carbon synthons, *Green Synth. Catal.*, 2023, **4**, 258–262.
55 X. Gao, T.-J. Han, B.-B. Li, X.-X. Hou, Y.-Z. Hua, S.-K. Jia, X. Xiao, M.-C. Wang, D. Wei and G.-J. Mei, Catalytic asymmetric dearomatization of phenols *via* divergent intermolecular (3 + 2) and alkylation reactions, *Nat. Commun.*, 2023, **14**, 5189.
56 T. J. Han, Z. X. Zhang, M. C. Wang, L. P. Xu and G. J. Mei, The Rational Design and Atroposelective Synthesis of Axially Chiral C2-Arylpyrrole-Derived Amino Alcohols, *Angew. Chem., Int. Ed.*, 2022, **61**, e202207517.
57 Y.-W. Li, N.-N. Mo, H. Zhang, J.-X. Wu, T.-J. Han, X. Xiao, D. Wei and G.-J. Mei, Organocatalytic asymmetric synthesis of Tröger's bases, *Nat. Commun.*, 2025, **16**, 6383.
58 D. A. Lenev, K. A. Lyssenko, D. G. Golovanov, V. Buss and R. G. Kostyanovsky, Bis-*ortho*-Substitution by Methyl Groups Dramatically Increases the Racemization Barrier of Tröger Bases, *Chem.–Eur. J.*, 2006, **12**, 6412–6418.
59 D. A. Lenev, I. I. Chervin, K. A. Lyssenko and R. G. Kostyanovsky, Adducts of Tröger bases and activated acetylenes: synthesis and structure, *Tetrahedron Lett.*, 2007, **48**, 3363–3366.

60 H. Tian, F. Peng, P. Zhang, H. Yang and H. Fu, Highly Enantioselective Iridium-Catalyzed Cascade Double Allylation Strategy: Synthesis of Pyrrolidinoindolines with an All-Carbon Quaternary Stereocenter, *Org. Lett.*, 2019, **21**, 8501–8505.

61 H. Liu, Z. Sun, K. Xu, Y. Zheng, D. Liu and W. Zhang, Pd-Catalyzed Asymmetric Allylic Substitution Cascade of But-2-ene-1,4-diyl Dimethyl Dicarbonate for the Synthesis of Chiral 2,3-Dihydrofurans, *Org. Lett.*, 2020, **22**, 4680–4685.

62 C. Qian and W. Tang, A Versatile Synthesis of Vinyl-Substituted Heterocycles *via* Regio- and Enantioselective Pd-Catalyzed Tandem Allylic Substitution, *Org. Lett.*, 2020, **22**, 4483–4488.

63 X. Wang, H.-L. Mao, Y.-H. Yang, H. Jiang, L.-Q. Chen, S.-J. Tu, W.-J. Hao and B. Jiang, Regio- and Enantioselective Synthesis of Dihydropyrido[1,2-a]indoles *via* Catalytic Asymmetric Annulative Allylic Alkylation, *J. Org. Chem.*, 2022, **87**, 15644–15652.

64 L.-Q. Chen, C.-F. Zhu, S. Zhang, B.-Y. Liu, S.-J. Tu, W.-J. Hao and B. Jiang, Palladium-catalyzed annulative allylic alkylation for regioselective construction of indole-fused medium-sized cyclic ethers, *Chin. Chem. Lett.*, 2023, **34**, 108398.

65 C. Yuan, Y. Zhang, H. Xi and X. Tao, An acidic pH fluorescent probe based on Tröger's base, *RSC Adv.*, 2017, **7**, 55577–55581.

66 (*a*) CCDC 2390173: Experimental Crystal Structure Determination, 2025, DOI: **10.5517/ccdc.csd.cc2l75cd**; (*b*) CCDC 2446125: Experimental Crystal Structure Determination, 2025, DOI: **10.5517/ccdc.csd.cc2n3d8g**.